

Focal Plane Detectors for Dark Energy Camera (DECam)

J. Estrada¹, R. Alvarez², T. Abbott², J. Annis¹, M. Bonati², E. Buckley-Geer¹, J. Campa³, H. Cease¹, S. Chappa¹, D. Depoy⁴, G. Derylo¹, H. T. Diehl¹, B. Flaugher¹, J. Hao¹, S. Holland⁵, D. Huffman¹, I. Karliner⁶, D. Kubik¹, S. Kuhlmann⁷, K. Kuk¹, H. Lin¹, N. Roe⁵, V. Scarpine¹, R. Schmidt², K. Schultz¹, T. Shaw¹, V. Simaitis⁶, H. Spinka⁷, W. Stuermer¹, D. Tucker¹, A. Walker², W. Wester¹ for the Dark Energy Survey Collaboration

¹Fermi National Accelerator Laboratory, Illinois, USA

²Cerro Tololo Inter-american Observatory, La Serena, Chile

³Centro de Investigaciones Energeticas, Medioambientales y Tecnologicas-Madrid, Spain

⁴Texas A&M University, Texas, USA

⁵Lawrence Berkeley National Laboratory, California, USA

⁶University of Illinois at Urbana-Champaign, Illinois, USA

⁷Argonne National Laboratory, Illinois, USA

May 31, 2010

ABSTRACT

The Dark Energy Camera is an wide field imager currently under construction for the Dark Energy Survey. This instrument will use fully depleted 250 μm thick CCD detectors selected for their higher quantum efficiency in the near infrared with respect to thinner devices. The detectors were developed by LBNL using high resistivity Si substrate. The full set of scientific detectors needed for DECam has now been fabricated, packaged and tested. We present here the results of the testing and characterization for these devices and compare these results with the technical requirements for the Dark Energy Survey.

1. DECAM CCDS AND THE DES TECHNICAL REQUIREMENTS

The Dark Energy Survey (DES) is a project planning to map 5000 sq-deg of the southern galactic zap using a new imager to be installed on the prime focus of the the Blanco 4m Telescope at CTIO, in Chile. A general overview of this project is discussed in Ref.¹ and references therein. In order to accomplish the scientific goals for the survey an imager with a field of view of 3 sq-deg is under construction, scheduled to be completed early in 2011. The DECam focal plane is composed of 62 2k x 4k CCDs for producing the science images and 12 2k x 2k CCDs to be used for guiding and focusing.

The detectors to be used on the DECam focal plane have been produced and tested and are ready to be mounted on the imager. In this paper we present the technical requirements for the focal plane detectors on DES and discuss in detail some aspects of the charac-

terization done for these CCDs. Details of the DECam focal plane can be found in Ref.¹

The design of the DECam imager is optimized for DES which requires observation of galaxies up to redshift $z \approx 1.3$. This establishes strong specifications on the efficiency of the DECam detectors in the red and near-infrared range. Recent advances in CCD technology² allow the fabrication of high resistivity ($\sim 10k\Omega\text{cm}$) detectors, up to $\sim 300 \mu\text{m}$ thick which are fully depleted at relatively low voltages. These CCDs have a significantly higher efficiency in the near-IR and for this reason are the optical detectors chosen by several groups building new mosaic cameras for astronomy, such as DECam^{3,4} and HyperSuprime.⁶ This type of detectors was also selected by the SNAP team for their proposed instrument.⁵ The DECam CCDs are discussed in Refs.^{3,7,8,9}

A cartoon of the devices developed by Lawrence Berkeley National Laboratory (LBNL)² that are going to be used in the DECam focal plane is presented in Fig. 1. It is a back illuminated, p-channel CCD thinned to 250 μm and biased from the back side to be fully depleted. The charge collected in the depletion region is stored in the buried channels established a few μm away from the the gate electrodes. The holes produced near the back surface must travel the full thickness of the device to reach the potential well. The detectors to be used for science imaging have 2k x 4k pixels and two readout channels located at the end of a serial register divided in two halves. A flat exposure obtained for one of the DECam CCDs is shown in Fig. 2. The detectors used for guiding and focus will be the same type of CCDs but in a 2k x 2k format. These detectors have 15 μm x 15 μm pixels.

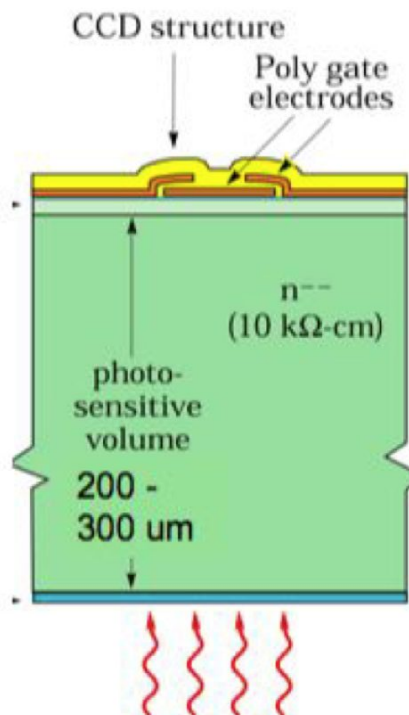


Figure 1. Schematic of a DECam detector. Back illuminated, 250 μm thick, p-channel CCD. For more details see Ref.²

The DES Collaboration has defined the requirements for the DECam CCD detectors, summarized in Table 1. They correspond mostly to standard requirements for astronomical CCDs with the exception of the average quantum efficiency in the near infrared denoted as the “z” filter, according to the Sloan Digital Sky Survey filter set.¹⁰

2. PACKAGING AND TESTING OF DECam DETECTORS AT FERMILAB

The DECam CCDs are produced by DALSA¹¹ and LBNL¹² and delivered to Fermilab as diced parts. Fermilab has developed a package for these CCDs that meets the mechanical and thermal requirements established by DES, the details of the DES package is discussed in Ref.¹³ The procedures and tools to build these packages were also developed at Fermilab and details are discussed in.¹³ A photography of the final version of the DECam science package is shown in Fig. 3

After each detector is packaged, it is installed on a single CCD testing station where all the DECam technical requirements are verified. An example of a testing station is shown in Fig. 4. The staged production testing of a DECam detector takes approximately

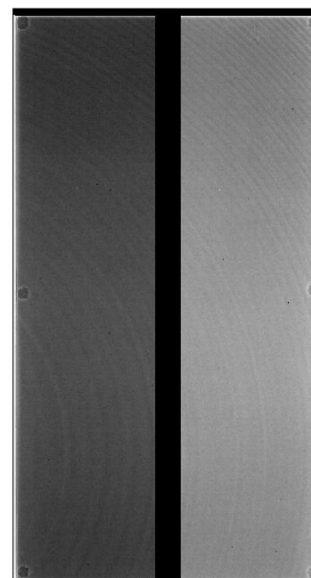


Figure 2. Flat exposure with a light level of $\approx 27,000 \text{ e}^-$. The serial register is divided in two and in this image the serial overscan is displayed on the center of the CCD. The parallel overscan is displayed on the top of the image. The 6 approximately square features on along the edges of the CCD correspond to the footprint of adhesive tape used for alignment during an intermediate packaging step. Also visible are the 0.5 % variations on the signal level produced by the rings of the resistivity variation on the silicon substrate, these features are completely removed after a flat field correction.

2 days. Fermilab has established a CCD testing lab with three fully instrumented testing stations for production testing. The CCD lab has also two additional testing stations, one dedicated to measure the mechanical properties of these CCDs¹³ and one dedicated to specific studies that are not part of the routine production testing. These stations are often also used to characterize the performance of the custom design DECam electronics.¹⁵

The CCD packaging and testing facilities at Fermilab have been able to maintain an average testing rate of 4 detectors a week. This was done early in the project to reduce the risk typically associated with producing such a large number of science grade CCDs. Thanks to this effort, the DECam CCD team has been able to produce all the scientific detectors needed more than 18 months before the scheduled first light for the instrument, and approximately 1 year before they are needed to start building the final focal plane. The details of the production testing facility and procedures are presented in Ref.¹⁴

Table 1. DECam technical requirements.

#	description specification
1	nonlinearity <1%
2	full well: >130,000 e ⁻
3	no residual image
4	readout time < 17 sec
5	dark current <35 e ⁻ /pix/hour
6	QE [g, r, i, z]: [60%, 75%, 75%, 65%]
7	QE < 0.5 % per degree K
8	read noise <15 electrons
9	Charge diffusion σ <7.5 μ m
10	Cosmetic defects < 0.5 %
11	Crosstalk for two amps. on CCD < 0.001.

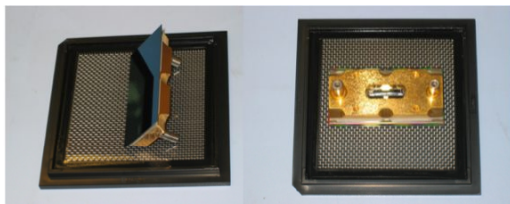


Figure 3. DECam science package. The CCD is attached to a gold plated invar foot with two alignment pins for mounting on the focal plane and a high density Airborne²³ connections for readout.

3. QUANTUM EFFICIENCY

The main feature distinguishing the DECam detectors from other CCDs is the quantum efficiency in the red and near-infrared. DES imaging will be performed in 4 filters according to the SDSS filter set¹⁰. The requirement on the "z" filter in Table 1 is the one that constitutes the biggest challenge, not commonly achieved for thinned CCDs. During our standard testing of these detectors we measure the QE for each device from 400 nm to 1080 nm. A typical result obtained from one of our CCDs is shown in Fig. 5 compared with the Site 2k x 4k detectors installed on the existing imager at the Blanco 4m Telescope prime focus (Mosaic II¹⁶).

In addition to requiring a high QE in the near-IR, DECam also needs relatively uniform and stable QE. This means that the QE on different detectors has to be similar. During the production testing of the DECam detectors we have obtained results that indicate very consistent QE among the science detectors, as shown in Fig. 6

The quantum efficiency for silicon detectors in the

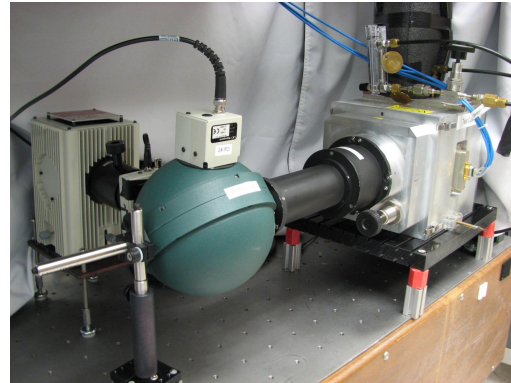


Figure 4. CCD testing station. A aluminum vacuum vessel with the shape of a cube (right) is used to facilitate quick detector exchange, the detector is cooled with an automated LN2 distribution system. A 6" integrating sphere is attached 13" from the front of the cube to produce and approximately flat illumination. A monochromator (not shown) is used to select the illumination wavelength.

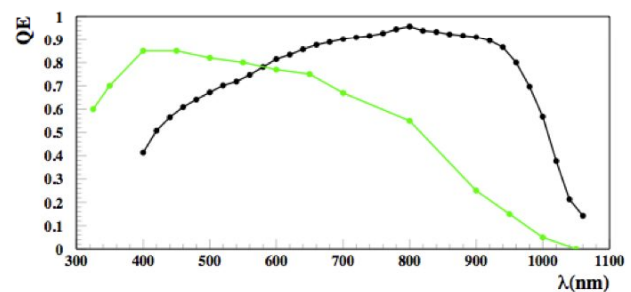


Figure 5. Quantum efficiency for a DECam CCD (black) compared with the QE for the SITE detectors currently installed in the prime focus imager of the Blanco Telescope.

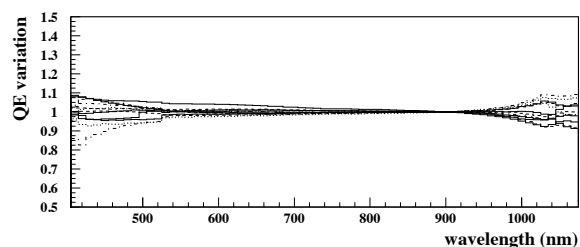


Figure 6. Quantum efficiency relative variations observed in a group of 12 representative DECam CCDs.

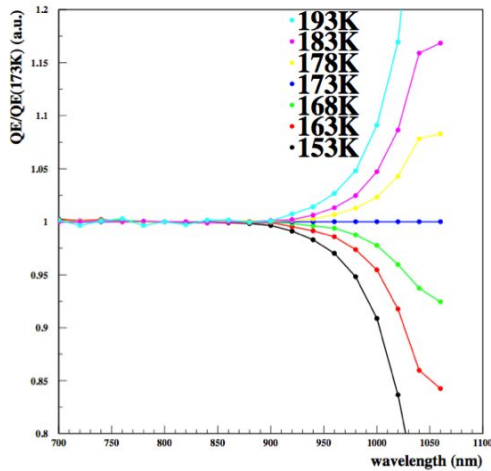


Figure 7. QE efficiency variations relative to the nominal operating temperature of 173 K.

near-IR depends strongly on temperature. A stable QE is needed for DES operations, which imposes a requirement on the temperature stability of the DECam focal plane. The QE for the DECam CCDs was studied as a function of temperature. The results are shown in Fig. 7. For a wavelength of 1000 nm, there is a temperature dependence coefficient of $\alpha = 0.5\%/^{\circ}\text{K}$. Given this factor, the QE stability requirement for DES translates into a temperature stability specification of variations smaller than 0.25°K during any period of 12 hours.

4. LATERAL CHARGE DIFFUSION

As mentioned above the DECam detectors achieve higher quantum efficiency than commonly used astronomical CCDs because they are $250\text{ }\mu\text{m}$ thick instead of the typical $30\text{ }\mu\text{m}$. This means that some charge is produced far away from the minimum potential well, where it is stored until readout. During their transit inside the depletion region, the charge carriers (holes) could also move in the direction perpendicular to the pixel boundaries. This effect, called charge diffusion, has to be kept under control in order to avoid a significant degradation in the image quality. The CCDs used in most astronomical instruments until now are thinned to $<30\text{ }\mu\text{m}$ to reduce the charge diffusion. For the DECam CCDs, a substrate voltage is applied to the back surface to control diffusion and obtain acceptable image quality. These detectors are fabricated on high-resistivity Si to allow for a full depletion with relatively low substrate voltages (40 V).

A tool commonly used in the characterization of CCD detectors is the exposure to X-rays from a ^{55}Fe source.¹⁷

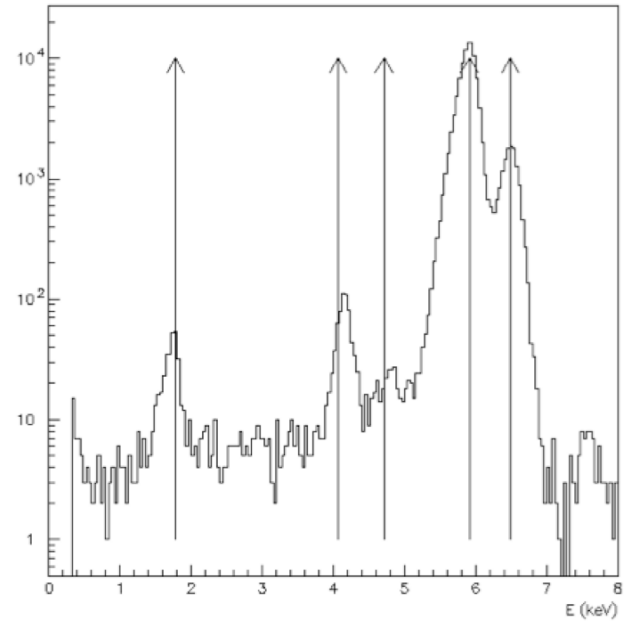


Figure 8. Spectrum obtained for the reconstructed X-ray hits in an ^{55}Fe exposure of a DECam CCD. The arrows are marking the direct X-rays from the source $K_{\alpha}=5.9\text{ keV}$ and $K_{\alpha}=6.5\text{ keV}$. The K_{α} and K_{β} escape lines at 4.2 and 4.8 keV, and the Si X-ray at 1.7 keV. The factor of 3.64 eV/e^{-} is used to convert from charge to ionization energy.

The main emission of the ^{55}Fe source is a 5.9 keV X-ray. An example of the energy spectrum seen in a DECam CCD is shown in Fig.9. The size of X-ray hits in a back illuminated CCD provides a measurement of the diffusion. A 5.9 keV X-ray produced by an ^{55}Fe source will penetrate only about $20\text{ }\mu\text{m}$ into the silicon before the producing a charge pair.¹⁷ The charge will have to travel most of the Si thickness before it can be stored under the potential well. As a result of this process, ^{55}Fe X-rays will produce in the detector hits with the size determined by the lateral diffusion.

The diffusion measurements for DECam CCDs, using X-rays is shown in Fig. 9. The size of the x-ray hits is measured in the CCD images by calculating the first order moments of the reconstructed events. This measurement done with X-rays is consistent with measurements using optical methods also done for DECam detectors¹⁸ and other thick detectors developed by LBNL^{19,20} The optical measurements are shown Fig.10. For these detectors we also measure the impact of the operating temperature on the lateral charge diffusion, and the results are shown in Fig.9

As an additional check of the image quality for DECam we built a star projector using a slow optical sys-

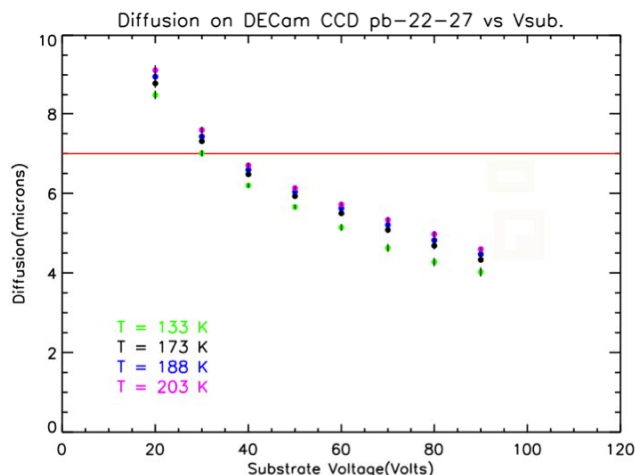


Figure 9. Diffusion measurement using X-rays from a ^{55}Fe source in a 250 μm DECam CCD with pixel size 15 μm x 15 μm .

tem and a 10 μm circular pinhole. The image of the pinhole was focused on the CCD surface. The image produced with this system is shown in Fig.11 and has a size of FWHM=1.57 pixels. Considering the DECam pixel scale of 0.27"/pixel, this would be equivalent to FWHM=0.4" better than the PSF expected on the best seeing conditions at the Blanco telescope.. The result of this test does not produce a measurement of diffusion because of the unknown the image quality of the optical system. However it is reassuring to see that these detectors are capable of producing images with the quality needed for the DES science goals.

5. EDGE EFFECTS

The field lines on the edges of the DECam detectors are slightly deformed as discussed in Ref.²¹ The effect extends the charge collection area for the edge pixels beyond the fiducial pixel region into the edge of the detector, a region occupied by a conductive ring structure used to shape the fields inside the device. For an exposure with flat illumination the edge pixels collect more light than the center pixels because of this effect. This is clearly visible in flat exposures for the science DECam CCDs shown in Fig.2. The magnitude of the glow observed on the flat exposures is presented in Fig.12.

For DES imaging the usable pixels are those that have less than 10% difference in effective collecting area compared with their neighbor, this comparison is done using light in a 10nm wide band around 900 nm. This definition establishes a region of about 8 pixels which will not be used for imaging as shown in Fig.12

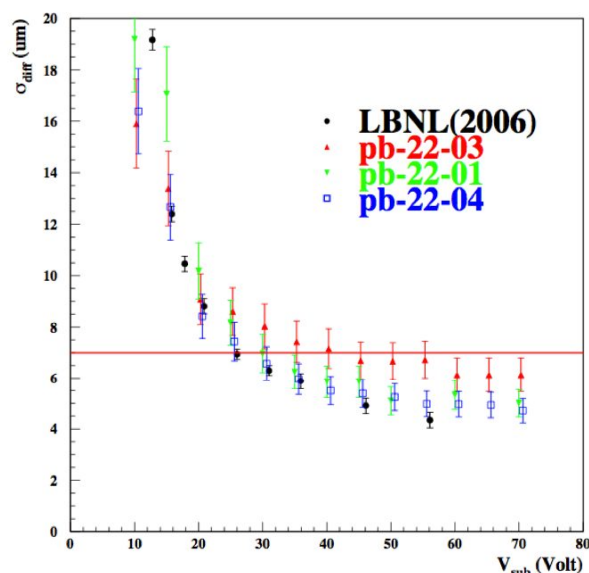


Figure 10. Diffusion measurement for the 250 μm thick DECam CCDs using an optical diffraction pattern.¹⁸ The black points represent the diffusion measurements done with the virtual knife edge technique^{19,20} for a similar detector with a thickness of 200 μm thick.

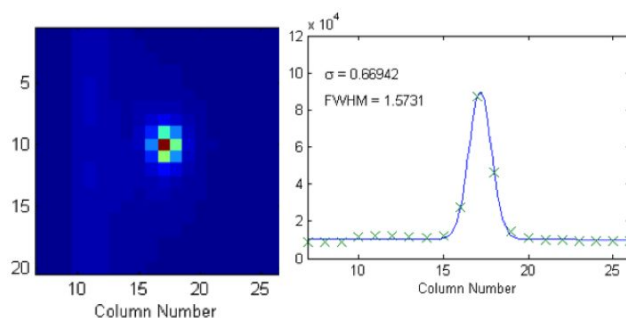


Figure 11. Left) image produced with a optical projector described in the text. Right) Profile of the image.

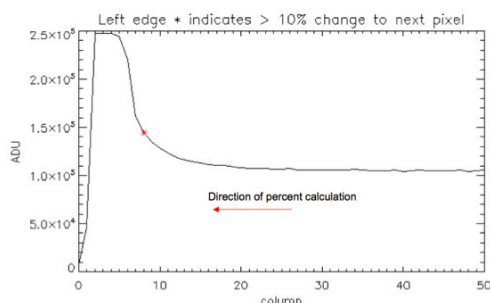


Figure 12. Profile near the edge for a flat exposures on a DECam CCD. The red point shows the limit on the usable area defined according to the DES requirements described on the text.

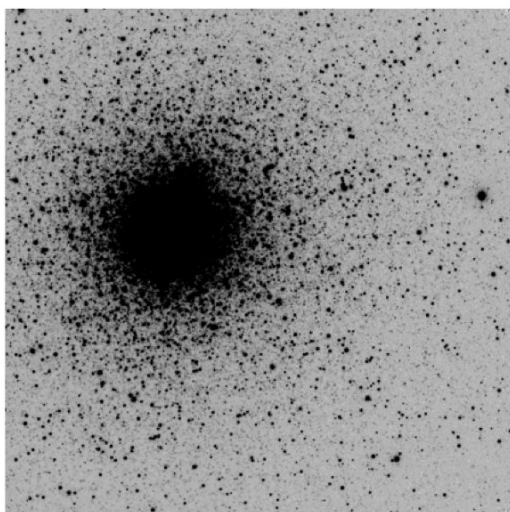


Figure 13. Imaging of the Tuc 47 globular cluster produced with a DECam CCD installed on a 1m telescope at CTIO.

The edge effect was also studied during one of our observing runs with engineering DECam CCDs performed at a 1m telescope in CTIO (details of these runs are discussed below). A globular cluster (Tuc 47) was imaged at different locations on the CCD as shown in Fig. 13. The reconstructed positions of the stars when the cluster was located on the center of the CCD were used as reference positions. The cluster was then moved towards the edge of the detectors and the offset for the observed stars was measured as a function of the location on the CCD. The results show the effect of the distorted pixels at the edge of the device. Fig. 14 shows the distortions measured in this way, compared to those expected from the flat field studies. The results are consistent.

The edge effect for DECam CCDs was also investigated using a collimated x-ray source with precision movement over the area of the CCD. This measure-

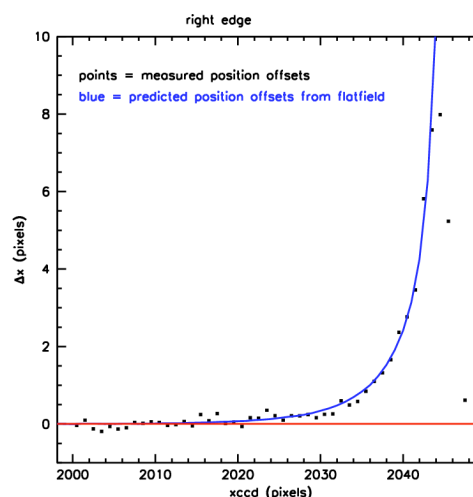


Figure 14. Distortions measured in flat field exposures for DECam CCDs (blue curve) compared to the distortions measured during the 1m imaging of the Tuc 47 globular cluster as discussed in the text (black points).

ments are discussed in Ref.²² and are consistent with the results shown in Fig. 14.

6. LINEARITY, NOISE AND FULL WELL CAPACITY

During production testing¹⁴ for DECam several photon transfer curves¹⁷ are collected for each CCD. They consist on taking exposures with flat illumination at different light levels going up to 200,000 e^- . Using this data the gain for the device is determined. This data is also useful to study the linearity in the response of the signal readout chain and the readout noise.

The gain is measured by looking at the linear relation between the variance on the image as a function of the mean. Given Poisson statistics a linear relation between these two quantities is expected. An example of a photon transfer curve produced during the production testing for a DECam CCD is shown in Fig.15. The gain is measured as the slope in Fig.15, in this case the gain for the detector is 0.9 ADU/ e^- . The curve also shows that the linear relation valid up to 175,000 ADU.

DECam requires its detectors to have a full well capacity larger than 130,000 e^- , and show less than 1% non-linearities up to those light levels. The data collected in the photon transfer curve is used to confirm this. Figure 16 shows the non-linearity measurements for a typical science grade CCDs and demonstrates the linear response of the complete readout system up to 225,000 e^- .

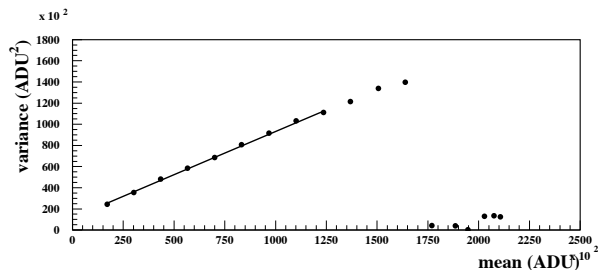


Figure 15. Variance as a function of mean signal obtained in a photon transfer curve during production testing of a DECam CCD.

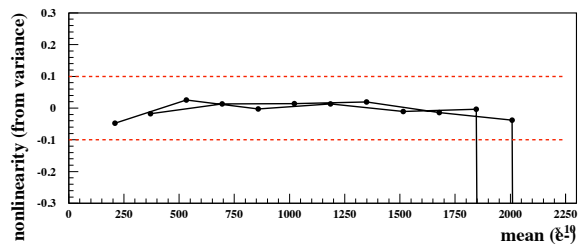


Figure 17. Non linearity measured in the variance vs mean curve shown in Fig.15.

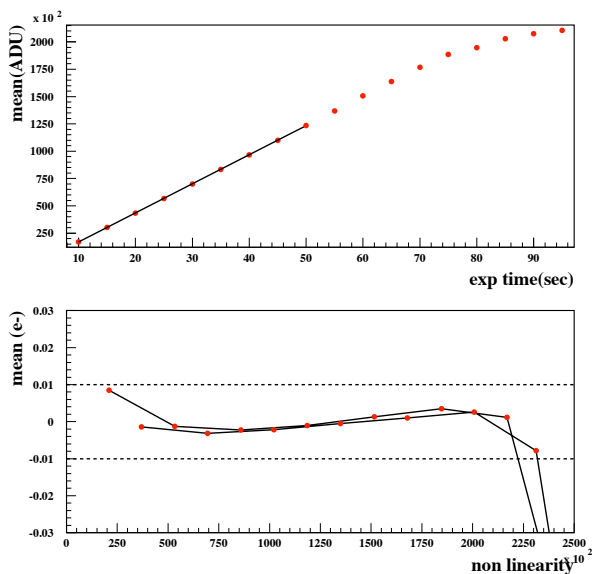


Figure 16. Top) Mean signal as a function of exposure time. Bottom) Fractional non-linearity on the upper panel as a function of mean signal. The 1% technical requirement for DECam is satisfied for signals up to 225,000 e^- .

Even with a demonstrated linear response above 200,000 e^- , the DECam detectors show an effect that reduces the maximum charge that can be reliably measured on a single pixel. The relation between variance and mean deviates more than 10% from linear at around 180,000 e^- as can be seen in Fig.17. We attribute this effect to a variation on the charge transfer efficiency (CTE) for high light levels. The CTE for the DECam science CCDs is required to be better than 0.99999, and it is checked for every single device using the EPER technique in flat exposures with 27,000 e^- and also X-rays, the results are not discussed here. However, when the light level is much larger ($\approx 180,000 e^-$) the CTE starts decreasing generating correlations between pixels that reduce the variance as seen in Fig.17.

The data presented in Fig.16 does not give much information about the performance of the readout system at low light levels. For this reason a separate linearity check specific to very low light levels is produced. This is shown in Fig. 18, which again demonstrates a non-linearity well below the 1% requirement for DECam.

From previous work done by other groups we know that the linearity for the CCD itself could be much better than 1%. The measurements presented in Fig.16 and Fig. 18 could be overestimating the non-linearities due to fluctuations on the light source or on the shutter timing. To produce more precise measurement, the linearity in the response on one side of the detector is compared with the other side, this would eliminate any systematic effect associated with the shutter or the light source. Since both sides are readout by independent signal paths this will check for any possible low level defects on one signal amplifier with respect to the other. The results of this measurement are shown in Fig. 19, and show that the two amplifiers follow each other with precision better than 0.1%.

To measure the noise a photon transfer curve at lower

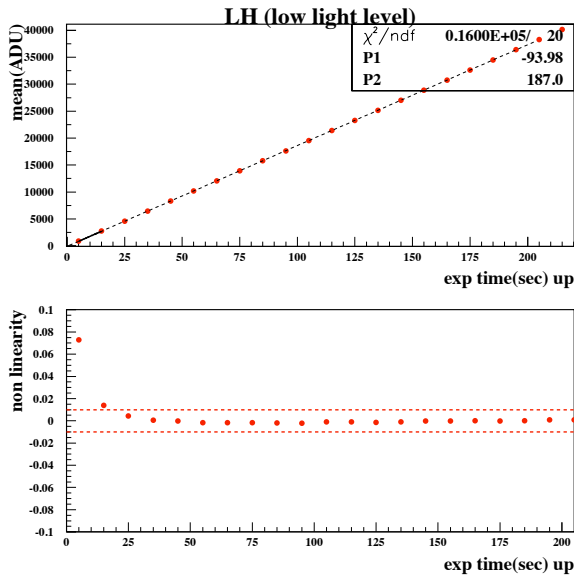


Figure 18. Low level nonlinearity measurement.

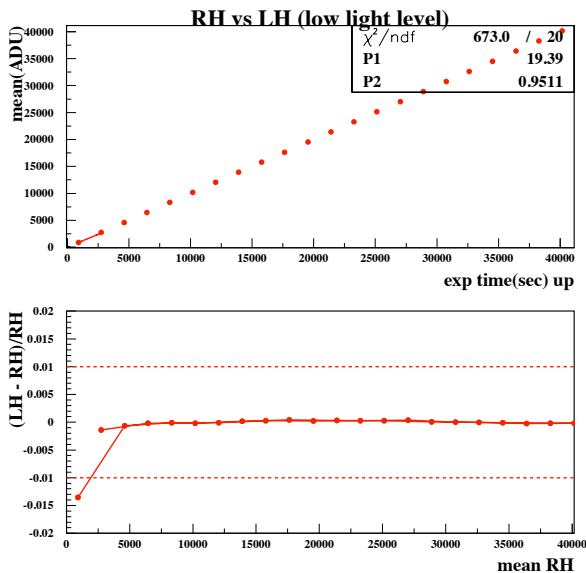


Figure 19. Non linearities in the relative response of the two signal path of a DECam CCD.

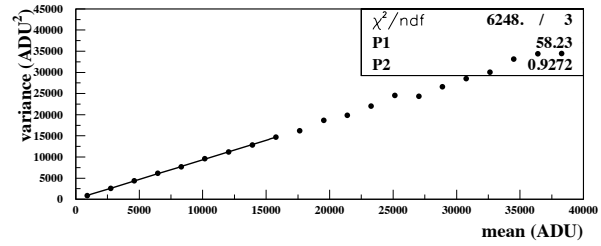


Figure 20. Low level photon transfer curve showing a gain of 0.93 ADU/e⁻ and a noise of 8.5 e⁻.

light level is produced, shown in Fig.20. This curve is fitted to obtain the linear relation between the variance and the mean. A good measurements of the variance for an image with no light is obtained, which corresponds to the readout noise for the detector. In this case $\sigma_0^2 = 58\text{ADU}^2$, which corresponds to a readout noise of $\sigma_0 = 7.6\text{ADU} = 8.5e^-$. The data presented here was collected with a pixel time of $4\mu\text{sec}$ per pixel which meets the DECam readout time and noise requirements.

The noise performance of these detectors has been studied in detail as part of the characterization effort done by the DECam CCD team^{7,8}. The signal is digitized after correlated double sampling (CDS) of the output. Each sample used for the CDS operation is the result of an integration during a time τ . This integration acts as a filter for high frequency noise. The noise measured for a DECam detector as a function of readout time is shown in Fig. 23. The noise observed for pixel readout times larger than $50\mu\text{s}$ is $\sigma < 2e^-$ (RMS). At large readout times, τ is one half of the pixel readout time. The detectors have an output stage with a electronic gain of $\sim 2.5\mu\text{V}/e^-$. These results were obtained using a Monsoon¹⁵ CCD controller.

7. SYSTEM TESTING

The DECam project built a Multi-CCD Test Vessel (MCCDTV) for system testing of these detectors, their readout electronics and the mechanical and thermal properties of the complete system. A photograph of the MCCDTV is shown in Fig.?? and details of testing done with it at discussed in Ref.²⁴. All the technical requirements for the detectors have been satisfied on the MCCDTV at the same level seen in the single CCD test station. A maximum of 28 engineering grade CCDs were installed on the MCCDTV and readout simultaneously.

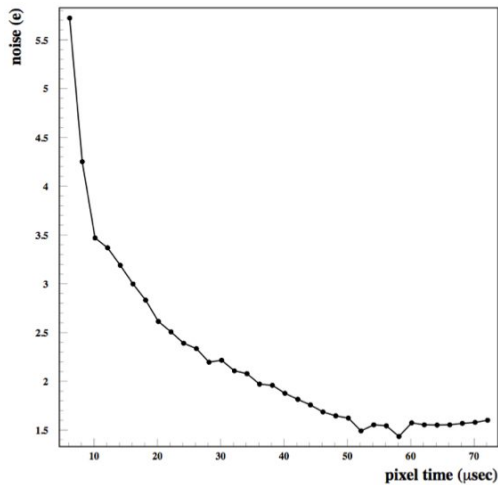


Figure 21. Noise as a function of pixel readout time for DECam CCDs. At slow readout speeds a noise below $\sigma = 2$ e is achieved.



Figure 23. Tarantula nebula VRI composite color image obtained on October 2008 using a DECam 2k x 2k CCD mounted on a 1m telescope at CTIO.

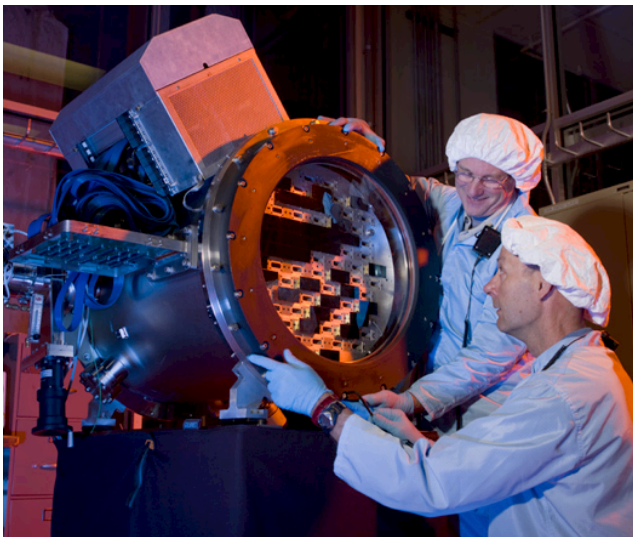


Figure 22. Multi CCD Test Vessel. This is a full size prototype focal plane partially instrumented with production DECam electronics.

The DECam detectors have not been extensively used before on astronomical instruments. Some test have been done before for imagers,² and some similar devices have been installed on spectrographs. As part of certification for the DECam CCDs observations were performed on a 1m telescope at CTIO²⁵. These tests served not only as a demonstration of the performance of the CCDs on the sky, but also as a test of the complete signal path for DECam on the mountain. The tests were done using science grade 2kx2k detectors installed on an engineering package. Observing runs of ≈ 6 nights were done every season starting on the first semester 2008. The final runs done on March 2010 used the DECam production readout system and the results demonstrated that the system can operate reliably on a telescope environment achieving the same performance seen on the lab.

In addition to the system testing on MCCDTV and the testing performed at the 1m CTIO telescope, the DECam detectors were also tested for long term reliability. An array of 4 2k x 2k CCDs was installed on a vacuum vessel and operated cold continuously for 13 months. The vacuum vessel was kept cold and dark exposures were produced every few hours. An example of a 10 hr dark exposure is shown in Fig.24. The gain, dark current level and readout noise for these detectors were monitored continuously showing stable results. After



Figure 24. Portion of an dark 40,000 sec exposure collected during the long term reliability test of DECam CCDs.

13 months the detectors were fully characterized using the standard DECam procedures and the results show no changes with respect to the characterization done before the long operation. These tests were done as part of an R&D effort for the possible application of CCDs in low background experiments.²⁶ The result of this test constitutes a reassuring demonstration of the long term reliability of the DECam detectors.

8. CONCLUSION

The DECam imager is currently being built for installation in the prime focus of the Blanco 4m Telescope at CTIO, Chile. This instrument will be used for the Dark Energy Survey that is scheduled to start operations on the second semester of 2011.

The focal plane detectors for the DECam instrument have been produced and characterized and are now waiting installation of the final focal plane. To achieve this goal the DECam project has established a new CCD packaging and testing facility at Fermilab that has operated continuously in production mode for about 2 years.

The DECam CCDs meet all the technical requirement established by the DES project. In many cases the detectors exceed this requirements by a large factor. In this work we presented the main features that make the DECam CCD special because of their thickness : i) quantum efficiency, ii) lateral charge diffusion and iii) edge distortions. We also discussed the readout noise, full well and linearity characteristic of these devices. All the test done so far indicate that the detectors will perform according to the DECam requirements.

The DECam project has done significant system testing for these detectors using three different approaches: i) full size prototype focal plane partially populated with engineering CCDs and in the CCD lab, ii) observing runs with a DECam CCD and electronics and iii) a long term stability study with an array of 4 CCDs

running continuously for more than 1 year. The results of all these system test are encouraging, indicating that the system design for DECam will perform according to the instrument requirements.

The DECam team plans to continue system tests using the MCCDTV and the DECam imager vessel with engineering grade CCDs for about 6 more months before starting to build the final focal plane with the detectors of scientific quality.

Acknowledgements

Funding for the DES Projects has been provided by the U.S. Department of Energy, the U.S. National Science Foundation, the Ministry of Science and Education of Spain, the Science and Technology Facilities Council of the United Kingdom, the Higher Education Funding Council for England, the National Center for Supercomputing Applications at the University of Illinois at Urbana-Champaign, the Kavli Institute of Cosmological Physics at the University of Chicago, Financiadora de Estudos e Projetos, Fundao Carlos Chagas Filho de Amparo Pesquisa do Estado do Rio de Janeiro, Conselho Nacional de Desenvolvimento Cientfico e Tecnolgico and the Ministrio da Cincia e Tecnologia, the German Research Foundation-sponsored cluster of excellence Origin and Structure of the Universe and the Collaborating Institutions in the Dark Energy Survey.

The Collaborating Institutions are Argonne National Laboratories, the University of California at Santa Cruz, the University of Cambridge, Centro de Investigaciones Energeticas, Medioambientales y Tecnologicas-Madrid, the University of Chicago, University College London, DES-Brazil, Fermilab, the University of Edinburgh, the University of Illinois at Urbana-Champaign, the Institut de Ciencies de l'Espai (IEEC/CSIC), the Institut de Fisica d'Altes Energies, the Lawrence Berkeley National Laboratory, the Ludwig-Maximilians Universitt, the University of Michigan, the National Optical Astronomy Observatory, the University of Nottingham, the Ohio State University, the University of Pennsylvania, the University of Portsmouth, SLAC, Stanford University, and the University of Sussex.

REFERENCES

- [1] Brenna Flaugher, SPIE2010 , to appear with these proceedings.
- [2] S.E. Holland, D.E. Groom, N.P. Palaio, R. J. Stover, and M. Wei, IEEE Trans. Electron Dev., **50** 225 (2003), LBNL-49992.

- [3] Flaugher, B., Ground-based and Airborne Instrumentation for Astronomy. Edited by McLean, Ian S.; Iye, Masanori. Proceedings of the SPIE, Volume 6269, (2006)
- [4] Dark Energy Survey Collaboration, astro-ph/0510346.
- [5] "Supernova / Acceleration Probe: A Satellite Experiment to Study the Nature of the Dark Energy", SNAP Collaboration, G. Aldering *et al.*, submitted to Publ. Astr. Soc. Pac., astro-ph/0405232; SNAP Collaboration, astro-ph/0507459.
- [6] M. Satoshi et al., Ground-based and Airborne Instrumentation for Astronomy. Edited by McLean, Ian S.; Iye, Masanori. Proceedings of the SPIE, Volume 6269, (2006)
- [7] J. Estrada & R. Schmidt , Scientific Detectors for Astronomy 2005, Edited by J.E. Beletic, J.W. Beletic and P. Amico, Springer, (2006).
- [8] J. Estrada et al. , Ground-based and Airborne Instrumentation for Astronomy. Edited by McLean, Ian S.; Iye, Masanori. Proceedings of the SPIE, Volume 6269, (2006).
- [9] H.T. Diehl et al., High Energy, Optical, and Infrared Detectors for Astronomy III, Edited by David A. Dorn and Andrew D. Holland. Proceedings of the SPIE, Volume 7021 (2008).
- [10] Fukugita, M. et al., Astronomical Journal v.111, p.1748 (1996)
- [11] <http://www.dalsa.com/>
- [12] <http://www-ccd.lbl.gov/>
- [13] Derylo et al., Proceedings of the SPIE, Volume 6276, pp. 627608 (2006)
- [14] Kubik, D. et al. , SPIE2010 , to appear with these proceedings
- [15] T. Shaw et al., SPIE2010 , to appear with these proceedings
- [16] <http://www.ctio.noao.edu/mosaic/>
- [17] J.R. Janesick, Scientific Charge Cupled Devices, SPIE press (2001).
- [18] H. Cease, H. T. Diehl, J. Estrada, B. Flaugher and V. Scarpine, Experimental Astronomy , Online First (2007)
- [19] J.A. Fairfield , D. E. Groom, S. J. Bailey, C. J. Bebek, S. E. Holland, A. Karcher, W. F. Kolbe, W. Lorenzon, & N. A. Roe, Fairfield IEEE Trans. Nucl. Sci. 53 (6), 3877 (2006)
- [20] A. Karcher, C.J. Bebek, W. F. Kolbe, D. Maurath, V. Prasad, M. Uslenghi, M. Wagner, IEEE Trans. Nucl. Sci. 51 (5), (2004) LBNL-55685.
- [21] S.E. Holland, W.F. Kolbe, and C.J. Bebek, Device Design for a 12.3 Megapixel, Fully Depleted, Back-Illuminated, High-Voltage Compatible Charged-Coupled Device, IEEE Trans. Electron Devices, vol. 56, no. 11, Nov. 2009.
- [22] Kuhlmann, S. et al, in preparation
- [23] <http://www.airborn.com/>
- [24] J. Hao et al, SPIE2010 , to appear with these proceedings
- [25] <http://www.astro.yale.edu/smarts/smarts1.0m.html>
- [26] Estrada et al., arXiv:0802.2872; Estrada et al., arXiv:0911.2668